Modeling of Asphalt and experiments with a discrete particles method

T.J. Ormel & V. Magnanimo & H. L. ter Huerne & S. Luding
Tire-Road Consortium, CTW, University of Twente, The Netherlands

ABSTRACT: Asphalt is an important road paving material. Besides an acceptable price, durability, surface conditions (like roughening and evenness), age-, weather- and traffic-induced failures and degradation are relevant aspects. In the professional road-engineering branch empirical models are used to describe the mechanical behaviour of the material and to address large-scale problems for road distress phenomena like rutting, ravelling, cracking and roughness. The mesoscopic granular nature of asphalt and the mechanics of the bitumen layer between the particles are only partly involved in this kind of approach. The discrete particle method is a modern tool that allows for arbitrary (self-)organization of the asphalt meso-structure and for rearrangements due to compaction and cyclic loading. This is of utmost importance for asphalt during the construction phase and the usage period, in forecasting the relevant distress phenomena and understand their origin on the grain-, contact-, or molecular scales. Contact models that involve visco-elasticity, plasticity, friction and roughness are state-of-the art in fields like particle technology and can now be modified for asphalt and validated experimentally on small samples. The ultimate goal is then to derive micro- and meso-based constitutive models that can be applied to model behaviour of asphalt pavements on the larger macro-scale.

1 INTRODUCTION

Asphalt mixtures are composite materials that consist of solid particles, viscous binder/fluid (bitumen) and pores filled with air. When considering asphalt we should distinguish different states the mixture can be in: a) hot and non-compacted (construction phase, relatively loose particle matrix) and b) compacted at ambient temperature. During compaction of the mixture the relative contents of the different phases changes: starting from the initially loose material, the particle in the skeleton move close to each other and air in the voids is squeezed out. The fluid in the mixture (that can be hot or cold, i.e. less or more viscous) lubricates the contact surfaces between the particles and can make movement of the particles easier 0. The multiphase material has properties that depend on those of the original components, i.e. aggregate and binder. The physical properties of the skeleton (e.g. shape, surface texture, size distribution, moduli), but also the properties of the binder (e.g. grade, relaxation characteristics, cohesion) and binder–aggregate interactions (e.g. adhesion, absorption, physiochemical interactions) characterize the material behavior of the asphalt mixture. In addition, aggregate particles in the mixture have different shapes, surface texture and orientations, which make the description of the contacts between particles a challenge (Zhong 1999).

When looking at asphalt, it makes sense to distinguish between three different length scales, i.e. micro-, meso- and macro-scale. The interaction between the mortar (composition

of bitumen and the smallest particles) and a single large stone is defined as the micro-scale. The interaction of multiple stones of various sizes and the mortar is defined as the meso-scale. On the macro-scale, the behavior of the whole road is accounted for. Kinematics at different scales apparently governs the behavior of the material: to gain thorough knowledge of asphalt pavement behavior, one has to focus on all three length scales. As common practice in the professional asphalt branch, fundamental constitutive models able to describe the micro- and meso-mechanical behavior are hardly used. Large scale problems are addressed by using empirical models 0 for road distress phenomena like rutting, raveling, cracking and roughness. The mesoscopic granular nature of asphalt, the chemistry and the mechanics of the (modified) bitumen layer between the particles is, because of the limitations of those empirical models, just partly involved. Our ambitious goal is to bridge the gap between discrete and continuous concepts. The material behavior at the grain-scale can be combined with the granular structure in order to identify the contact law for the asphalt components and relate such kinematics with the macroscopic response at the larger scale of the road. Finding a micro-based model with predictive quality on the macro-level is the ultimate challenge.

On the particle-scale, the interaction of the mortar with the grains and between the grains can be efficiently investigated using a Discrete Element Method (DEM) 0. Discrete element methods simulate particulate systems by modeling the translational and rotational degrees of freedom of each particle using Newton's laws, and the forces are calculated associating proper contact models with each particle contact.

In the last twenty years, attempts for a micro-mechanical modeling of asphalt have been done by other researchers: a contact law for the behavior of two particles connected by a binder and elastic to describe the behavior of an assembly of bonded particles was proposed in Ref. 0; a micro-mechanical description of rutting with intergranular and aggregate-binder interactions was given in Ref. 0; 2D modeling based on image processing are reported in 0. DEM studies on cemented particulate materials include the work by Rothenburg et al. 0, Chang and Meegoda 0, Sadd and Dai 0, Buttlar and You 0 and Ullidtz 0.

Nevertheless, a well-established multiscale description for the constitutive behavior of particle-bitumen systems is still missing. Particularly, very limited work has been done on 3D micro-mechanical modeling of the mixture, with proper visco-elasto-plastic, temperature-dependent contact/interaction models. Moreover, to our knowledge, no systematic numerical study on the microscopic processes that govern cracks (and eventually self-healing) in asphalt has been done. On the technological/methodological side, a general computational framework suitable for simulating the loading/cyclic and fracture/healing behavior of granular-bitumen composites is the need of the hour. The detection and analysis of damage as well as microscopic self-healing mechanisms have been achieved by particle based simulations already 0 so that these results now can be applied to asphalt and translated to a practicable continuum model with predictive quality, which will allow proposing and designing optimized materials with superior self-healing capabilities in the future 0.

In this preliminary study an approach to modeling of cohesive and sintering particulate materials is described 0. The mechanical evolution in time of all the particles in the material is simulated in DEM using a modern version of the sintering contact model 0. This contact model mimics the physical behavior of the interaction of the particles accounting for dissipative, elasto-plastic, adhesive, and frictional effects and the pressure dependence. The model is by construction non-linear in its response to external load 0. An additional temperature-dependence, as possibly resulting from diffusion of atoms and the resulting sintering effects, can be added on top of the elasto-plastic contact model 0.

Initially, some particle-samples are prepared by applying isotropic (hydrostatic) pressure. The spherical particles deform plastically at contact and stick to each other forming a solid sample with (after releasing pressure) zero confining stress – on which uni-axial unconfined tension or compression is further applied. In the last section uni-axial confined compression tests are compared to laboratory tests on Open Graded Asphalt. A systematic study is performed on the influence of the plasticity parameter and friction coefficient on the mechanical behavior of the numerical sample. Interestingly, when a proper plasticity parameter from experiments is inferred and adopted in the simulation, the experiments are in good agreement with the numerical curve, and the coefficient of friction alone is able to capture the differences in the material behavior due to different kind of bitumen.

2 DEM MODELING OF PARTICULATE MATERIALS

The Discrete Element Method (DEM) 0 for particle systems can be used to illustrate how the macroscopic response of a solid-like, sintered sample, resembling an asphalt mixture, depends on various micro- and meso-scopic properties such as the particle-particle contact network, the particle size, and the contact adhesion between particles (simulating the interaction of the bitumen with the particles), their contact friction and stiffness. In the present work, after solving the equations of motion at the particle level, the coupling between micro- and macro scale properties is performed. The response of the particle system (expressed in terms of macroscopic stress and strain) is obtained by averaging (0) the local quantities at the particle contact level (interparticle contact forces and displacements) over the assembly. The effective response then depends directly on the chosen particle contact model 000. Even though recent studies have demonstrated that the accurate simulation of systems composed of non-spherical particles is possible 00, for simplicity we restrict ourselves here to spherical particles.

2.1 *Adhesive contact model*

The non-linear model by Luding *et al.* 00,0 is used – see these references for more details, to describe the adhesive particle-particle interaction in the asphalt mixture. In Figure 1, the normal contact force f (that is directed parallel to the line connecting the centers of two contacting particles) is plotted against the contact overlap (resembling the deformation between particles at the contact), $\delta > 0$. If $\delta < 0$, there is no contact between particles, and thus $f = 0$. This sign convention relates positive (*negative*) values of the contact displacement δ to overlap/deformation (*separation*), while positive (*negative*) values of the contact force f relate to compression/repulsion (*tension*/*attraction*).

A contact begins at $\delta = 0$ and, during initial compressive loading, the contact force increases with the overlap as $f = k_1\delta$, with k_1 the elasto-plastic contact stiffness. When the external compressive forces are compensated by the contact repulsive force at the maximum contact overlap, δ_{max}, for unloading, the contact stiffness increases to a value k_2, so that the elastic unloading force is $f = k_2(\delta - \delta_f)$. Elastic unloading to zero contact force leads to the (plastic) contact overlap $\delta_f = (k_2 - k_1)\,\delta_{max}/k_2$. If the overlap is further decreased, the contact force gets tensile, with maximum tensile contact force $f_{t,max} = -k_t\delta_{t,max}$, realized at contact displacement $\delta_{t,max}$. For the sake of brevity, the tensile softening parameter k_t hereafter is referred to as the "contact adhesion".

The k_2 value depends on the maximum overlap, that is the model accounts for an increasing stiffness with deformation. The maximum overlap and the limit contact stiffness k_2 are related through

$$\delta_{max} = \frac{k_2}{k_2 - k_1}\phi\frac{2a_1a_2}{a_1 + a_2}, \tag{1}$$

with the dimensionless plasticity depth, ϕ , defined relative to the reduced radius. If the overlap is larger than a fraction ϕ of the particle radius (for $a_1 = a_2$), the (maximal) constant stiffness k_2 is used. Note that, when the limit defined by ϕ is reached, the contact stiffness suddenly increases from k_1 to the much higher value k_2; at the same time the behavior switches from elasto-plastic to perfectly elastic along the k_2 branch. These characteristics of the model very well resemble the multiphase nature of asphalt mix, in which a softer bitumen layer surrounds hard stone particles. During loading, first the elasto-plastic adhesive layer of bitumen is compressed. Later, when the deformation increases further, the hard (stiffer) stone core get compressed and a new elastic resource is encountered. Then, the plasticity parameter

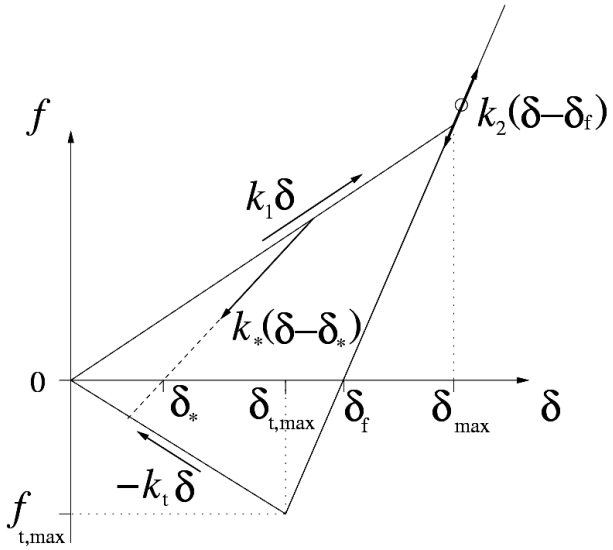

Figure 1. Particle contact model plotted as force-displacement relation (Luding2008b), with δ for contact positive, and repulsion and attraction forces positive and negative, respectively.

ϕ can be seen as a measure of the thickness of the bitumen layer relative to the radius of the particles.

The extreme loading and unloading limit branches are reflected by the outer triangle in Figure 1. Starting from the realized maximal overlap, $\delta^*_{max}<\delta_{max}$, unloading occurs within the outer triangle, as characterized by a branch with stiffness $k_*=k_1+(k_2-k_1)\,\delta_{max}{}^*/\delta_{max}$, and (elastic, reversible) force, $f^*=k_*(\delta-\delta^*)$. The intermediate stiffness k_* follows from a linear interpolation between k_1 and k_2 – which is our (arbitrary) choice due to the lack of experimental data on this (probably) non-linear behavior. In summary, the model has three ("stiffness") *k*-parameters that describe the three relevant physical effects at the contact: (1) elasticity, (2) plastic deformations, and (3) contact-adhesion. Furthermore, the model involves (4) a non-linear contact stiffness via the choice of k_*. This piece-wise linear model is a compromise between simplicity and the need to model physical effects. Except for some early theoretical studies, see 0 and the many works that are based on it, there is no experimental/numerical literature available to our knowledge that provides enough detailed information on the force-displacement relations, involving all four physical contact properties above and their nonlinear, history-dependent behavior. If this information becomes available, the present model can be extended and generalized.

The *tangential contact force* acts parallel to the particle contact plane and is related to the tangential contact displacement through a linear elastic contact law, with the tangential stiffness k_s. The tangential contact displacement depends on both the translations and rotations of the contacting particles. Coulomb friction determines the maximum value of the tangential contact force: During sliding the ratio between the tangential contact force and the normal contact force is assumed to be limited and equal to a (constant) dynamic friction coefficient μ_d; during sticking, the tangential force is limited by the product of normal force and static coefficient of friction μ_s.

3 RESULTS: UNI-AXIAL UNCONFINED TEST

In this section we report results from uni-axial unconfined tests after isotropic preparation of the sample. The detailed explanation of the numerical protocol is an useful introduction to the next section on confined uni-axial compression, where we compare the simulations with physical experiments.

The simulations reported here consist of two different stages, namely a sample preparation stage (isotropic compression) and an uni-axial (tensile or compressive) loading stage. Six plane, perpendicular outer walls form a cuboidal volume, with side lengths of $L=62.1$ mm. The samples are composed of about 10^3 poly-disperse spherical particles (see Fig. 2 as an

example), with particle radii drawn from a Gaussian distribution around mean $\overline{R}=2.7\,\mathrm{mm}$ 0,0). The particle density used in the simulations is ρ=2328 kg/m^3, the maximum elastic contact stiffness is $k_2=10^7$ kg/s. The initial elasto-plastic stiffness (normalized by k_2) is $k_1/k_2=1/2$, and the contact adhesion k_t/k_2 is varied. The other stiffness parameters, friction coefficients, and viscous damping parameters are summarized in Table I, most of them being dimensionless, like all quantities discussed in the rest of the paper. As final remark, we note that the choice of parameters is empirical – most of them kept fixed here, only adhesion is varied systematically.

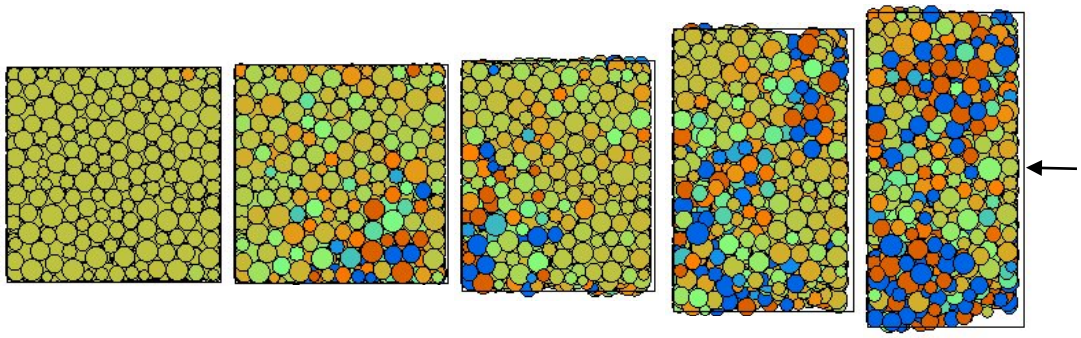

Figure 2. Sequence of snapshots from a compression test with poly-disperse particles and rigid outer walls (kt/k2=0.5). The circles are the particles with the greyscale coding the average stress.

Table I: Microscopic material parameters, rescaled as indicated in the right column. Using the dimensional parameters in column 4, for a collision of two particles of average size, with stiffness k_2 and viscosity γ_n, the contact duration becomes t_c=9.73ms with coefficient of restitution r=0.953 and the stress data presented in Figure 3 will be scaled by unit stress $\sigma_u=m_u/(x_u\,t_u^2)=3.704\ 10^6$ kg/(ms^2).

Property	Symbol	Values (Luding2008)	SI units
Time Unit	t_u	1	9.573 ms
Length Unit	x_u	1	0.54 m
Mass Unit	m_u	1	183.29 kg
Average radius	$\overline{R}$	0.005	2.7 mm
Material density	ρ	2	2328 kg/m³
Elastic stiffness	$k = k_2$	5	10^7 kg/s²
Plastic stiffness	k_1 / k_2	0.5	
Adhesion “stiffness”	k_t / k_2	[0, …, 20]	
Friction stiffness	k_s / k_2	0.1	
Plasticity range	ϕ_f	0.05	
Coulomb friction	$\mu = \mu_d = \mu_s$	1	
Normal viscosity	$\gamma = \gamma_n$	5.10^{-5}	0.9573 kg/s
Tangential viscosity	γ_t / γ	0.2	
Background viscosity	γ_b / γ	4	
Background torque	γ_{br} / γ	1	

3.1 *Isotropic Loading*

In this section the sample preparation by *pressure sintering* 0) is reported. During sintering, the particles deform plastically at contact and stick to each other due to strong, non-linearly increased van der Waals forces. At the same time, the sample shrinks, i.e. becomes denser. Such pressure-sintering results in a solid sample with bonded particles, similar to asphalt mixtures. Moreover, the sintering model can be temperature-dependent, resembling the effect of the temperature in the asphalt preparation with bitumen 0. The process is characterized by

two stages: the first stage reflects the application of a hydrostatic (or isotropic) pressure, $\sigma_s/\sigma_0 = 4.10^{-2}$ (or $\sigma_s = 37\,\mathrm{N/mm^2}$) to a loose assembly of particles, with the reference stress $\sigma_0 = k_1/(2\overline{R})$. This desired isotropic stress is slowly applied to the six outer walls. The hydrostatic loading process is considered to be finished when the kinetic energy of the sample is negligible compared to the potential energy. For our sample, the solid volume fraction (volume of the solid particles over total volume) at the end of the hydrostatic loading process is $\nu = 0.676$, which relates to a porosity (volume of fluid and air phases with respect to total volume, in the specific case of asphalt) of $1-\nu = 0.324$.

The second stage of the pressure sintering process is reflected by a *stress relaxation* phase, where the external hydrostatic pressure is strongly reduced, while the adhesion between particles is now made different then zero. Due to the presence of particle contact adhesion, the lateral stability of the specimen remains preserved when the hydrostatic pressure is released, i.e., a coherent and stable particulate structure is obtained that can be subsequently used in the analysis of damage and healing under uni-axial loading conditions. The solid volume fraction of the sample after stress relaxation is decreased to $\nu = 0.63$.

3.2 *Response under uni-axial compression and tension*

In the uni-axial compression (tension) test, one of the two outer walls, with its normal parallel to the axial (loading) direction, is slowly moved towards (away from) the opposite wall (see Fig. 2). The change of the wall displacement in time is prescribed by a cosine function with rather large period in order to limit inertia effects.

The response of the sample under uni-axial compression and uni-axial tension is shown in Figure 3. The normal axial stress σ, is plotted as a function of the normal axial strain ε, where positive stress (*strain*) values relate to compression (*contraction*). The stress-strain curves are depicted for different values of k_t (normalized by k_2), which quantifies the adhesion at the particle contacts, see Figure 1. A larger particle contact adhesion increases the effective strength of the sample, both under uni-axial tension and compression. Furthermore, the overall strain at which the effective stress reaches its maximum increases with increasing contact adhesion, k_t.

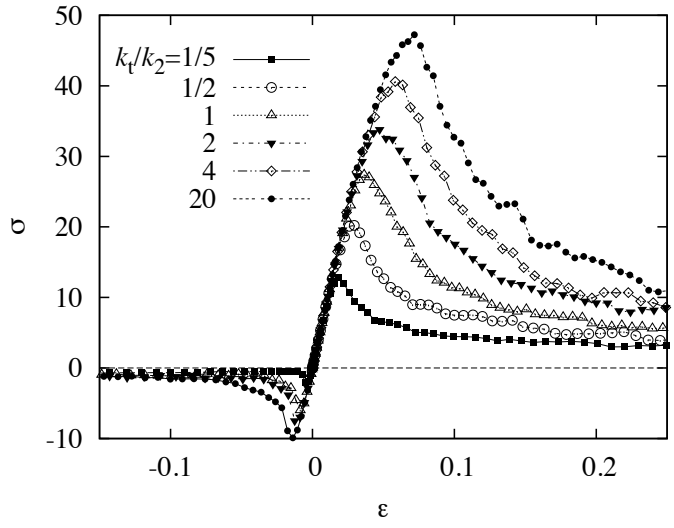

Figure 3. Axial stress [N/mm^2] plotted against axial strain during uni-axial compression (positive stress and strain values) and uni-axial tension (negative stress and strain values), for different particle contact adhesions k_t/k_2 (after (Luding2008b)).

Note that the maximum stress under uni-axial compression is order of five times larger than under uni-axial tension. A relatively high compressive strength in relation to the tensile strength is typical of various sintered materials, such as ceramics (Lee1995), and appears even in asphalt mixtures (Muraya2007). As further result, from Figure 3, the softening branch

under uni-axial tension is somewhat steeper than under uni-axial compression. The initial loading branch is linear up to large stress and the initial (elastic) axial stiffnesses G_t=962 N/mm^2 in tension and compression are determined by the sample preparation procedure, and are approximately equal for all the cases considered here, i.e., G_t/σ_0 = 1.04. The tensile responses are all characterized by local failure at the center of the sample. Note that the high axial stiffness is due to isotropic overcompression, while in the following section a different preparation procedure is applied.

4 RESULTS: UNI-AXIAL CONFINED TEST

4.1 *Laboratory experiments*

In order to make a parametric study of our numerical model, we compare uniaxial confined compression laboratory tests and simulations.

In the tests an open Open Graded Asphalt mixture is used, which consists of different sized aggregates, sand, fillers and bitumen. Open Graded Asphalt is a porous asphalt mix formulated to provide large voids (in excess of 20%) and allow surface water to drain away. This kind of mixture is continuously graded (in agreement with our numerical sample) and derives its stability from the packing of the aggregates and the cohesion provided by the bitumen. Tests are performed with two different types of bitumen: hot bitumen, which is also used during pavement construction and "*fake bitumen"*, a oil-based bitumen, that has properties, at room temperature, comparable to those of normal hot bitumen at compaction temperature (ter Huerne2008).

Tab. II: Initial properties of the laboratory samples. The solids density is the quantity that enters the simulations and the actual volume fraction is astonishingly close to the volume fraction for frictionless spheres.

Sample type	Symbol	Hot bitumen	Oil
Initial sample height [mm]	h_0	63,90	66,66
Total mass sample [gr]	m_0	999,00	1000,00
Initial volume sample [mm3]	V_0	635179,98	662639,83
Initial density [gr/mm3]	ρ_0	0,00157	0,00151
Amount of aggregate in sample [gr]	m_a	819,94	820,76
Volume of mastic in sample [mm3]	V_m	-	118510
Volume of aggregate in sample [mm3]	V_a	310818,80	311129,64
Volume percentage of solids [%]	-	-	64,84
Solids density [gr/mm3]	ρ_{a+m}	0,00157	0,002328
Volume percentage of aggregate [%]	-	51,07	46,95

Initially, the asphalt mix is blended so that the bitumen, together with the fine aggregates, is spread equally around the aggregates. The samples properties are resumed in Table II. Thereafter, the uni-axial compaction experiments are performed in a cylindrical steel mold with inner radius 112.5 mm, and inner height 150 mm, located under a press. On the top of the mix a stamp is placed (5277 gr), which is in contact with the force-measuring device of the press. The asphalt is compressed by letting the bottom plate of the press moving upwards, with constant velocity equal to 0.8 mm/s. The displacement of the bottom plate is also recorded. The experiment stops when the maximum force, 50 kN, is reached. The maximum possible stroke of the bottom plate is 30 mm.

The experiments are compared with DEM simulations of uni-axial confined compression tests on a granular poly-disperse mixture of 1331 spheres, modeled as described in Section 2. Details of the numerical parameters are resumed in Table III. The simulation starts with an isotropic system of particles, with initial solid volume fraction $\nu = 0.50$, resembling asphalt in a slightly compacted solid state. Then the sample is compressed by slowly moving the top wall downwards to a target strain ε=0.2 and then released by moving the same wall upwards. The total force that the particles are exerting on the fixed (bottom) wall is measured and compared with the laboratory tests in a stress strain plot.

In this study we performed a preliminary parametric study, to investigate which quantities have to be tuned in order to mimic the asphalt behavior. It follows that both coefficients of friction and plasticity play an important role. The first one allows to mimic the effect of bitumen strength, as it influences the (self-)reorganization of the particles. That is different kind of bitumen can be reproduced with different friction coefficients μ. On the other hand, the plasticity range ϕ is a measure of the average thickness of the layer of bitumen surrounding the solid particles relative to the average radius of the particles themselves, as explained in Section 2. The content of bitumen in the asphalt sample can be then resembled by ϕ.

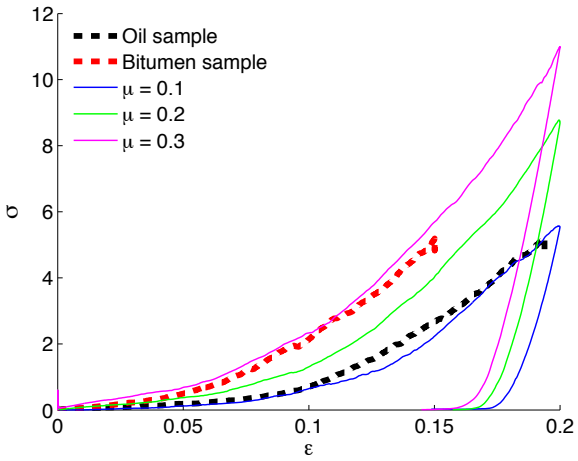

Figure 5. Stress [N/mm^2] versus strain in confined uni-axial compression tests: comparison between experiments (hot bitumen and oil) and simulation with different friction coefficients (μ increases for the curves going from the bottom to the top).

Here, we focus on these two parameters to match the physical experiments on Open Asphalt, keeping the other numerical parameters constants, see Table III. In particular, we calculated the *"equivalent ϕ"* in the laboratory samples as

$$\phi = \frac{3}{4}\frac{V_0 - V_a}{\pi \bar{R}^3} \tag{2}$$

with the N number of spheres in the numerical sample. For both experiments, we get a similar value for the plasticity range $\phi \approx 0.1$ and we use it as input parameter in our simulations. In Figure 5, we plot the stress-strain behavior for the uni-axial compression experiments and the numerical simulations performed with different friction coefficients $\mu = 0.1, 0.2, 0.3$. Despite the different procedure between the laboratory and numerical tests, the comparison shows that the elasto-plastic adhesive contact model is able to reproduce very well the basic features in the behavior of the asphalt mixture. Two regimes appear in the experiments: a slow increase for $\varepsilon < 0.1$ and a further transition to a much stiffer behavior when $\varepsilon > 0.1$. The same transient behavior is present in all the numerical curves. Moreover, the differences between the two laboratory samples, seems to be very well captured by only tuning the friction coefficient in the simulations, and keeping a constant ϕ, in agreement with the calculation made on the experimental samples.

5 CONCLUSIONS

In this work we studied adhesive granular samples under (1) uni-axial unconfined deformation after isotropic overcompression, and (2) uni-axial confined compression using DEM simulations with the final goal of application to asphalt mixtures.

(1) After isotropic overcompression, uni-axial compression/tension was applied to the sample for different contact adhesion strengths. While the initial stiffness (slope of the stress-strain curves) is not much affected, the peak strength of the material is: the stronger the

contact adhesion, the larger the peak strength. For compression, the strength appears about a factor of five larger than for tension and the softening branch is rather smooth for compression, while the tensile regime shows a sharper drop, resembling more brittle-like behavior.

(2) In contrast, the uni-axial confined compression tests did not suffer of overcompression, which makes the initial stress response much softer. When compared to laboratory tests on Open Graded Asphalt, this preparation procedure leads to encouraging agreement. The results show that in the our DEM model (i) the plasticity parameter can effectively reproduce the thickness of the bitumen layer relative to the average dimension of the stone particles in the real asphalt sample, (ii) the friction coefficient is able to mimic the influence of different kinds of filler (bitumen/oil) on the (self-) reorganization of the particles.

This preliminary work shows how powerful DEM simulations can be in describing the constitutive behavior of asphalt mixtures. In fact, discrete simulations give insights on the material microstructure and link observable (macroscopic) phenomena with the kinematics of the interacting components. Very useful information can be extracted from such microscopic analysis, e.g. on how and when to induce self-healing in a damaged material. Finally, given proper parameters from DEM simulations of element tests, a specific constitutive behavior can be implemented in a FE code to describe macro-scale process like rolling compaction.

Table III: Microscopic material parameters in the simulation of confined compression tests of Section 4. The third column gives the dimensionless variables as used in the simulations, while the fourth column provides the scaled variables in SI-units. The present scaling implies that stress values from simulations have to be multiplied by a factor of 10^5 Pa.

Property	Symbol	Values	SI units
Length Unit	x_u	1	1 m
Mass Unit	m_u	1	1.164 kg
Time Unit	t_u	1	0.003412 s
Average radius	$\overline{R}$	0.0027	2,7 mm
Material density	ρ	2000	2328 kg/m^3
Elastic stiffness	$k = k_2$	100	10^7 kg/s^2
Plastic stiffness	k_1 / k_2	1/5	
Adhesion “stiffness”	k_t / k_2	1/5	
Friction stiffness	k_s / k_2	1/5	
Plasticity range	ϕ_f	0.1	
Coulomb friction	$\mu = \mu_d = \mu_s$	0.1,0.2, 0.3	
Normal viscosity	$\gamma = \gamma_n$	1. 10^{-3}	0.3411 kg/s
Tangential viscosity	γ_t / γ	0.1	
Background viscosity	γ_b / γ	0.1	
Background torque	γ_{br} / γ	0.1	

REFERENCES

Alonso-Marroquin, F., Luding, S., Herrmann, H. J., and Vardoulakis, I. 2005. Role of anisotropy in the elastoplastic response of a polygonal packing, *Phys. Rev. E,* 71: 051304.

Buttlar, W.G., You, Z. 2001. Discrete element modeling of asphalt concrete: micro-fabric approach, *TRR*, 1757: 111–118.

Chang, G.K., Meegoda, N.J. 1993. Simulation of the behavior of asphalt concrete using discrete element method. In *Proc.2nd Int. Conf. Discr. Element Meth.*, MIT, 437–448.

Cundall P.A. and Strack O.D.L. 1979. A discrete numerical model for granular assemblies, *Géotechnique,* 29: 47–65.

D'Addetta, G. A., Kun, F., Ramm, E. 2002. On the application of a discrete model to the fracture process of cohesive granular materials, *Granular Matter* 4(2): 77-90.

Herbst, O., Luding, S. 2008. Modeling particulate self-healing materials and application to uni-axial compression, *Int. J. of Fracture* 154: 87-103.

Lee, W. E., Rainforth, W. M. 1995. *Ceramic Microstructures, Property Control by Processing,* Chapman and Hall, London, UK, 1995.

Luding, S. 2004 Micro-macro transition for anisotropic, frictional granular packings, *International Journal of Solids and Structures,* 41: 5821-5836.

Luding, S., Manetsberger, K., Muellers, J. 2005. A discrete model for long time sintering, *Journal of the Mechanics and Physics of Solids* 53(2): 455-491.

Luding, S. 2008. Cohesive, frictional powders: contact models for tension, *Granular Matter* 10: 235-246.

Luding, S., Suiker, A. 2008. Self-healing of damaged particulate materials through sintering, *Philosophical Magazine* 88 (28-29): 3445-3457.

Luding, S., and Bauer, E. 2010. Evolution of swelling pressure of cohesive-frictional, rough and elasto-plastic granulates. In *Geomechanics and Geotechnics: From Micro to Macro*, IS-Shanghai Conference Proceedings, 11.-12. Oct. 2010, M. Jiang, L. Fang, and M. Bolton (Eds.), CRC Press/Balkema, NL, 495-499.

Luding S. 2011. From discrete particles to solids - about sintering and self-healing (Review), *Comp. Methods in Mater. Science* 11(1): 53-63.

Muraya P.M. 2007. *Permanent deformation of asphalt mixes,* Ph.D. thesis – Delft University of Technology.

Rothenburg, L., Bogobowicz, A., Haas, R. 1992. Micro-mechanical modeling of asphalt concrete in connection with pavement rutting problems. In *Proceedings of the 7th International Conference on Asphalt Pavements I*, 230-245, 1992.

Sadd, M.H., Dai, Q. 2005. A comparison of micro-mechanical modeling of asphalt materials using finite elements and doublet mechanics, *Mechanics of Materials* 37: 641-662.

ter Huerne H. L., van Maarseveen M. F. A. M., Molenaar A. A. A., and van de Ven M. F. C. 2008. Simulation of HMA compaction by using FEM, *Int. J. Pavement Engineering* 9(3):153-163.

Thornton, C., Antony, S. J. 2000. Quasi-static deformation of a soft particle system, *Powder Technology* 109: 179-191.

Tomas, J. 2001. Assessment of mechanical properties of cohesive particulate solids – part 1: particle contact constitutive model, *Particle Science Technology* 19: 95-110.

Ullidtz, P. 2001. A study of failure in cohesive particulate media using the discrete element method. In *Proc. 80th TRB Meeting*, Washington, DC.

Van der Zwaag S. 2007. An introduction to material design principles: Damage prevention versus damage management. In: *Self Healing Materials. An Alternative Approach to 20 centuries of Materials Science*, Van der Zwaag ed., Springer, Dordrecht, NL, 1-18.

Zhong X. and Chang C.S. 1999. Micro-mechanical modeling for behavior of cementitious granular materials, *ASCE Journal of Engineering Mechanics*, 125(11): 1280-1285.